and/or heat sources were involved in the formation history of these objects. □

Received 21 May; accepted 21 July 2004; doi:10.1038/nature02882.

1. Alexander, C. M. O'D., Boss, A. P. & Carlson, R. W. The early evolution of the inner solar system: A meteoritic perspective. *Science* **293,** 64–68 (2001).
2. MacPherson, G. J. in *Meteorites, Comets and Planets* (ed. Davis, A. M.) 201–246, Vol. 1 of *Treatise on Geochemistry* (eds Holland, H. D. & Turekian, K. K.) (Elsevier-Pergamon, Oxford, 2003).
3. Rubin, A. E. Petrologic, geochemical and experimental constraints on models of chondrule formation. *Earth Sci. Rev.* **50,** 3–27 (2000).
4. Shu, F. H., Shang, H., Gounelle, M., Glassgold, A. E. & Lee, T. The origin of chondrules and refractory inclusions in chondritic meteorites. *Astrophys. J.* **548,** 1029–1050 (2001).
5. Russell, S. S., Srinivasan, G., Huss, G. R., Wasserburg, G. J. & MacPherson, G. J. Evidence for widespread ^{26}Al in the solar nebula and constraints for nebula time scales. *Science* **273,** 757–762 (1996).
6. Kita, N. T., Nagahara, S. & Morishita, Y. A short duration of chondrule formation in the solar nebula: Evidence from Al-26 in Semarkona ferromagnesian chondrules. *Geochim. Cosmochim. Acta* **64,** 3913–3922 (2000).
7. Huss, G. R., MacPherson, G. J., Wasserburg, G. J., Russell, S. S. & Srinivasan, G. Aluminum-26 in calcium-aluminum-rich inclusions and chondrules from unequilibrated ordinary chondrites. *Meteorit. Planet. Sci.* **36,** 975–997 (2001).
8. Mostefaoui, S. *et al.* The relative formation ages of ferromagnesian chondrules inferred from their initial aluminum-26/aluminum-27 ratios. *Meteorit. Planet. Sci.* **37,** 421–438 (2002).
9. Hsu, W. B., Huss, G. R. & Wasserburg, G. J. Al-Mg systematics of CAIs, POI, and ferromagnesian chondrules from Ningqiang. *Meteorit. Planet. Sci.* **38,** 35–48 (2003).
10. Amelin, Y., Krot, A. N., Hutcheon, I. D. & Ulyanov, A. A. Lead isotopic ages of chondrules and calcium-aluminium-rich inclusions. *Science* **297,** 1678–1683 (2002).
11. Adachi, I., Hayashi, C. & Nakazawa, K. Gas drag effect on elliptic motion of a solid body in primordial solar nebula. *Prog. Theor. Phys.* **56,** 1756–1771 (1976).
12. Busso, M., Gallino, R. & Wasserburg, G. J. Nucleosynthesis in asymptotic giant branch stars: Relevance for Galactic enrichment and solar system formation. *Annu. Rev. Astron. Astrophys.* **37,** 239–309 (1999).
13. Goswami, J. N. Short-lived nuclides in the early solar system: the stellar connection. *New Astron. Rev.* **48,** 125–132 (2004).
14. Sahijpal, S., Goswami, J. N., Davis, A. M., Grossman, L. & Lewis, R. S. A stellar origin for the short-lived nuclides in the early Solar System. *Nature* **391,** 559–561 (1998).
15. Wasserburg, G. J., Gallino, R., Busso, M., Goswami, J. N. & Raiteri, C. M. Injection of freshly synthesized ^{41}Ca in the early solar nebula by an asymptotic giant branch star. *Astrophys. J.* **440,** L101–L104 (1995).
16. Marhas, K. K., Goswami, J. N. & Davis, A. M. Short-lived nuclides in hibonite grains from Murchison: Evidence for Solar System evolution. *Science* **298,** 2182–2185 (2002).
17. Galy, A., Young, E. D., Ash, R. D. & O'Nions, R. K. The formation of chondrules at high gas pressures in the solar nebula. *Science* **290,** 1751–1753 (2000).
18. Urey, H. C. The cosmic abundances of potassium, uranium, and thorium and the heat balances of the Earth, the Moon and Mars. *Proc. Natl Acad. Sci. USA* **41,** 127–144 (1955).
19. Srinivasan, G., Goswami, J. N. & Bhandari, N. ^{26}Al in eucrite Piplia Kalan: plausible heat source and formation chronology. *Science* **284,** 1348–1350 (1999).
20. Bischoff, A. & Keil, K. Al-rich objects in ordinary chondrites: Related origin of carbonaceous and ordinary chondrites and their constituents. *Geochim. Cosmochim. Acta* **48,** 693–709 (1984).
21. Itoh, S. & Yurimoto, H. Contemporaneous formation of chondrules and refractory inclusions in the early Solar System. *Nature* **423,** 728–731 (2003).
22. Amelin, Y., Krot, A. & Twelker, E. Pb isotopic age of the CB chondrite Gujba, and the duration of the chondrule formation interval. *Geochim. Cosmochim. Acta* **68** Abst. E958 (2004).
23. Briceño, C. *et al.* The CIDA-QUEST large-scale survey of Orion OB1: Evidence for rapid disk dissipation in a dispersed stellar population. *Science* **291,** 93–96 (2001).
24. Podosek, F. A. & Cassen, P. Theoretical, observational, and isotopic estimates of lifetime of the solar nebula. *Meteoritics* **29,** 6–25 (1994).
25. Weidenschilling, S. J., Marzari, F. & Hood, L. L. The origin of chondrules at jovian resonances. *Science* **279,** 681–684 (1998).
26. Desch, S. J. & Connolly, H. C. A model of the thermal processing of particles in solar nebula shocks: Application to the cooling rates of chondrules. *Meteorit. Planet. Sci.* **37,** 183–207 (2002).
27. Sanders, I. A. in *Chondrules and the protoplanetary disk* (eds Hewins, R. H., Jones, R. H. & Scott, E. R. D.) 327–334 (Cambridge Univ. Press, Cambridge, 1996).
28. McDonough, W. F. & Sun, S.-S. Composition of the Earth. *Chem. Geol.* **120,** 223–253 (1995).
29. Galy, A. *et al.* Magnesium isotope heterogeneity of the isotopic standard SRM980 and new reference materials for magnesium-isotope-ratio measurements. *J. Anal. Atomic Spectrometry* **18,** 1352–1356 (2003).
30. Richter, F. M., Davis, A. M., Ebel, D. S. & Hashimoto, A. Elemental and isotopic fractionation of type B calcium-, aluminum-rich inclusions: Experiments, theoretical considerations, and constraints on their thermal evolution. *Geochim. Cosmochim. Acta* **66,** 521–540 (2002).

Supplementary Information accompanies the paper on **www.nature.com/nature**.

Acknowledgements Financial support for this project was provided by the Danish Lithosphere Centre (funded by the Danish National Science Foundation). M.B. is grateful for financial support in the form of an NSERC postdoctoral fellowship. We thank A. Halliday for his review of this paper.

Competing interests statement The authors declare that they have no competing financial interests.

Correspondence and requests for materials should be addressed to M.B. (mbi@dlc.ku.dk).

Exceptional astronomical seeing conditions above Dome C in Antarctica

Jon S. Lawrence[1], Michael C. B. Ashley[1], Andrei Tokovinin[2] & Tony Travouillon[1]

[1]*School of Physics, University of New South Wales, New South Wales 2052, Australia*
[2]*Cerro-Tololo Inter American Observatory, Casilla 603, La Serena, Chile*

One of the most important considerations when planning the next generation of ground-based optical astronomical telescopes is to choose a site that has excellent 'seeing'—the jitter in the apparent position of a star that is caused by light bending as it passes through regions of differing refractive index in the Earth's atmosphere. The best mid-latitude sites have a median seeing ranging from 0.5 to 1.0 arcsec (refs 1–5). Sites on the Antarctic plateau have unique atmospheric properties that make them worth investigating as potential observatory locations. Previous testing at the US Amundsen-Scott South Pole Station has, however, demonstrated poor seeing, averaging 1.8 arcsec (refs 6, 7). Here we report

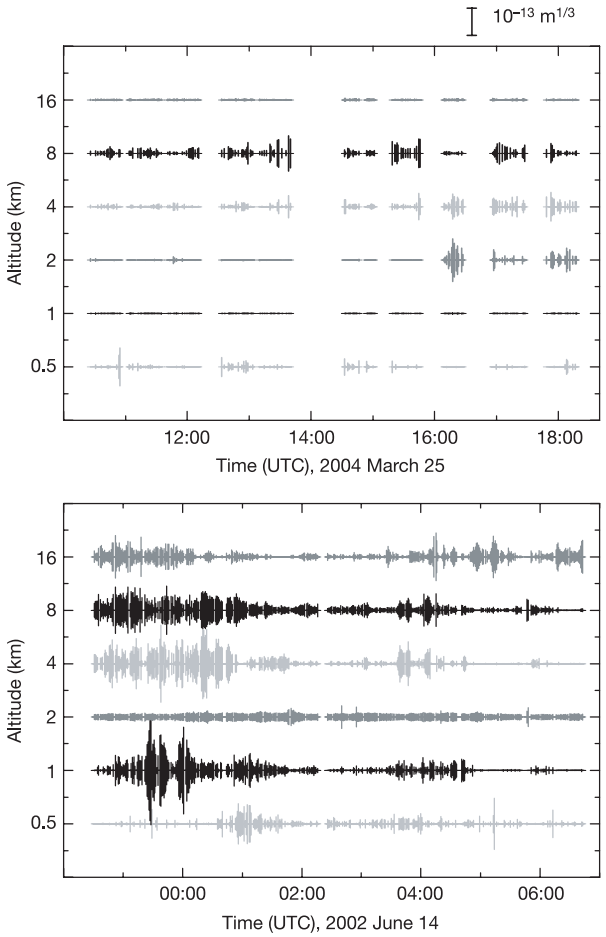

Figure 1 Comparison of turbulence profiles obtained from similar instruments at Dome C and Cerro Tololo. A typical night (representing ~50th percentile conditions) of the refractive index structure constant profile for Cerro Tololo[28] (bottom panel) and Dome C (top panel). Data are from similar MASS instruments. The length of the vertical bars at each altitude represents the magnitude of the refractive index structure constant integrated over that layer.

observations of the wintertime seeing from Dome C (ref. 8), a high point on the Antarctic plateau at a latitude of 75° S. The results are remarkable: the median seeing is 0.27 arcsec, and below 0.15 arcsec 25 per cent of the time. A telescope placed at Dome C would compete with one that is 2 to 3 times larger at the best mid-latitude observatories, and an interferometer based at this site could work on projects that would otherwise require a space mission.

In searching for sites for a major observatory, many factors need to be considered, including the atmospheric turbulence, cloud cover, precipitable water vapour, thermal emission from the atmosphere, auroral activity, aerosol/dust pollution, average and maximum wind speeds, seismic activity, rates of snow/rain fall, light pollution, accessibility, infrastructure and cost of operation. It has long been recognized that sites on the Antarctic plateau excel in many of these characteristics[9–11]. However, the poor seeing at the South Pole itself, caused by a highly turbulent layer of air within 200–300 m of the ground[12], is a major limitation. It has been postulated that such a turbulent layer may be absent at Dome C, owing to the local topography, lower wind speeds and higher altitude (3,250 m, compared to 2,840 m)[13,14]. Seeing measurements from Dome C during the 2003–04 summertime (daytime in Antarctica) have eliminated sources of local turbulence that had affected earlier measurements[15] and have now demonstrated periods of superb seeing below 0.2 arcsec (E. Aristidi and E. Fossat, personal communication). Summertime balloon-borne experiments have shown low levels of high-altitude winds[16]. However, the crucial information that astronomers need, and that we provide here, are measurements of the seeing in the wintertime, after sunset. Obtaining this data presented a formidable technical challenge, given that the French/Italian station at Dome C is currently uninhabited during winter[8], and that infrastructure such as electrical power and communications is not available.

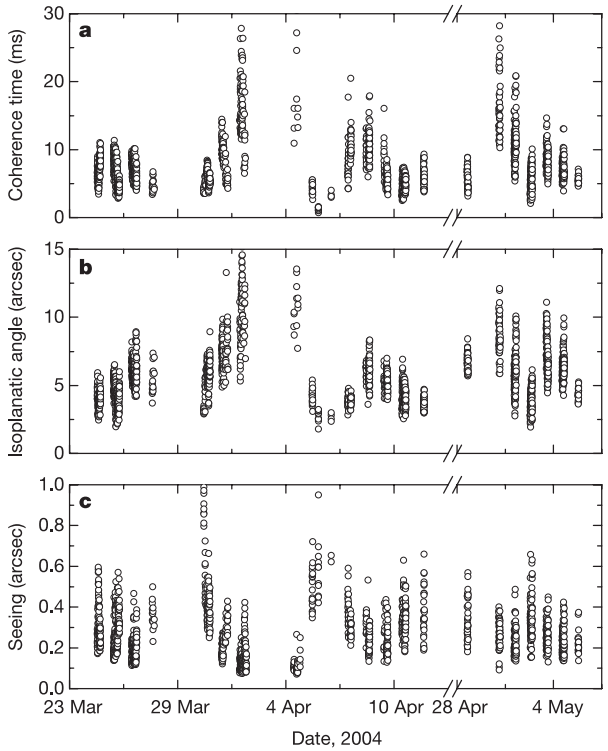

Figure 2 Dome C atmospheric coherence time, isoplanatic angle and seeing data as a function of time. Coherence time (**a**) and isoplanatic angle (**b**) are derived from the MASS instrument. Atmospheric seeing above 30 m (**c**) is computed from a combination of the refractive index structure constants from MASS and SODAR. Data covers the period 23 March to 5 May 2004. All data refer to observations at 1–1.5 airmass scaled to the zenith, and at a wavelength of 500 nm.

To obtain data over the winter months, we developed a remote autonomous laboratory, the AASTINO (Automated Astrophysical Site Testing International Observatory)[17]. This observatory was constructed at Dome C in January 2003, and it provides heat, electrical power, Iridium satellite communications, and computer control for a series of site testing instruments. In January 2004, we installed a Multi-Aperture Scintillation Sensor (MASS)[18] to measure the wintertime seeing. MASS uses the spatial/temporal structure of single star scintillation (that is, intensity fluctuations) to evaluate vertical refractive index fluctuation profiles[19,20]. The advantage of MASS over other techniques for measuring the seeing is that MASS uses a small telescope (making it less costly, and easier to automate) and it is able to measure the contributions to the seeing from six layers within the atmosphere, at fixed altitudes of 0.5, 1, 2, 4, 8 and 16 km. A limitation of MASS is that it is insensitive to seeing below about 500 m. We have therefore simultaneously used a SODAR (Sonic Detection And Ranging) instrument to determine the contribution from the layer between 30 and 500 m. From the MASS profiles, the 'free-atmosphere' seeing (above 500 m) and the isoplanatic angle (the angle over which atmospheric phase fluctuations are coherent) can be determined, and have been well-verified against other techniques (J. Vernin, A. Ziad and A.T., manuscript in preparation). The atmospheric coherence time (defined as the time over which the phase fluctuations are coherent) can also be derived from MASS, although the validity of this derivation for a complete range of atmospheric conditions is yet to be fully confirmed[21]. A MASS is currently in operation at Cerro Tololo[19] and several more are being deployed to other sites as part of a global site-testing effort.

The Dome C SODAR has been calibrated against microthermal sensors[22]. Robust performance of this instrument under Antarctic winter conditions, and good agreement with DIMM (Differential Image Motion Monitor) measurements, have previously been demonstrated through operation at the South Pole[12]. The calibration of the SODAR instrument is also significantly simplified in the low absolute humidity environment on the Antarctic plateau.

Figure 1 compares a typical night's profile of the refractive index structure constant (which describes the refractive index variations) from the Dome C MASS and a similar MASS instrument at the Cerro Tololo Inter American Observatory in Chile. The Tololo atmosphere, typical of mid-latitude sites, exhibits strong turbulence within the lower troposphere, extending up to 1 km above the surface. Additionally, strong turbulence is observed throughout the upper troposphere bounded by the jet stream at 10–14 km above the surface. The Dome C turbulence profile is quite different, and is unlike any observed at mid-latitude sites. The strongest turbulent

Table 1 **Comparison of observatory site conditions**

Site	ϵ_0	θ_0	τ_0
Dome C	0.27	5.7	7.9
South Pole	1.8	3.2	1.6
Mauna Kea	0.5–0.7	1.9	2.7
San Pedro Martir	0.59	1.6	6.5
Cerro Paranal	0.80	2.6	3.3
La Palma	0.76	1.3	6.6

ϵ_0 is the seeing in arcseconds, θ_0 is the isoplanatic angle in arcseconds and τ_0 is the coherence time in milliseconds. All values are corrected to the zenith and at a wavelength of 500 nm. Seeing, isoplanatic angle and coherence time at South Pole are mean total atmosphere values (above ground-level) from 16 microthermal balloon launches in winter 1995 combined with microthermal tower measurements of the 0–30 m ground layer[7]. Seeing and isoplanatic angle values at Mauna Kea, Hawaii are based on 20 nights of SCIDAR observations in 1995 (seeing above ground level)[1], and FWHM measurements from the Auto Guider of the Subaru telescope during focus checks over a 12 month period from 2000 to 2001 (seeing above ~15 m)[4]. Seeing from San Pedro Martir, Mexico, is the median from 2 yr of DIMM measurements (seeing above 8 m)[3]. Isoplanatic angle and coherence time from San Pedro Martir are obtained with generalized SCIDAR (located 15 m above ground level) over 27 nights in 1997 and 2000[29]. Seeing and isoplanatic angle from Cerro Paranal, Chile, are average values from DIMM measurements (above 5 m) over 10 yr (1989–95 and 1998–2002)[2]. The coherence time at Cerro Paranal is derived (to an accuracy of 20%) from DIMM measurements combined with balloon-borne wind speed measurements[2]. Seeing from La Palma, Canary Islands, is from 9 months of DIMM measurements (seeing above 5 m)[5]. Isoplanatic angle and coherence time from La Palma are from six microthermal balloon launches[30] in 1990.

layer occurs at a lower altitude owing to the lower tropopause height (5–8 km above the surface), and is of lower intensity owing to the lack of strong winds at this altitude. The only mechanism for turbulence generation in the Antarctic stratosphere above 10 km is from the Antarctic polar vortex, a system of strong high-altitude winds circling the continent[23]. Prior to our MASS data, it was a matter for speculation to what extent the vortex winds would affect the turbulence at Dome C. Our data show no evidence thus far of such turbulence.

The low values of high-altitude turbulence at Dome C lead to refractive index variations that are coherent over a large angle (that is, large isoplanatic angle) and over a long time (that is, large coherence time), see Fig. 2. The average values, 5.7 arcsec and 7.9 ms respectively, are higher than average values recorded at any other site, as shown in Table 1.

Combining the refractive index structure constant values for the free atmosphere determined by the MASS, with the surface boundary layer turbulence determined by the SODAR, gives the atmospheric seeing above 30 m (Fig. 2, Table 1). Whereas the surface boundary layer (within a few hundred metres of ground level) is usually a significant contribution to the total atmospheric seeing at mid-latitude sites, the 30–900 m turbulence observed at Dome C by the SODAR is exceptionally low, and is typically below the SODAR detection threshold (0.05 arcsec). This is expected from the very low-velocity ground level winds at this site. An additional contribution to the total atmospheric seeing is expected from the first 30 m above ground level (a region in which the SODAR is not sensitive).

A histogram of the atmospheric seeing above 30 m is shown in Fig. 3, and is compared to the probability distribution for seeing at Mauna Kea and Cerro Paranal. The mean Dome C seeing of 0.27 arcsec is only observed at mid-latitude sites under exceptionally calm conditions ($\ll$ 1% of the time). The best seeing we observed at Dome C was 0.07 arcsec, which, to our knowledge, represents the lowest value reported anywhere.

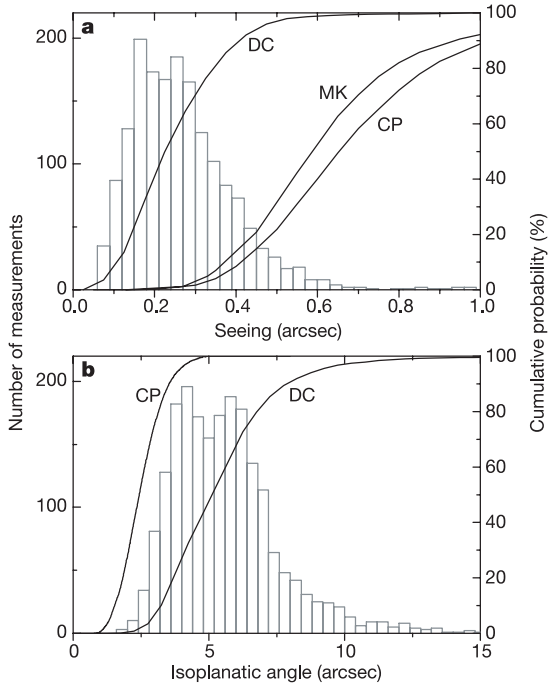

Figure 3 Histograms and cumulative distributions of the atmospheric seeing and the isoplanatic angle. **a**, Histogram of Dome C seeing above 30 m from MASS combined with SODAR, and cumulative distributions of seeing at Dome C (DC), Mauna Kea (MK) (derived from ref. 4), and Cerro Paranal (CP)[2]. **b**, Histogram of Dome C isoplanatic angle derived from the MASS instrument, and the cumulative distribution of isoplanatic angle from Dome C and Cerro Paranal[2].

The atmospheric characteristics of a site strongly influence the degree of correction and field of view achievable by using adaptive optics (AO)[24,25]. A factor of 4–10 fewer actuators would be required on a Dome C AO system to achieve the same residual wavefront error as a mid-latitude system. The larger isoplanatic angle of the Dome C atmosphere leads to a factor of ~3 increase in the field of view correctable by AO. The longer atmospheric time constant allows increased integration times for the AO wavefront sensor, which means that fainter guide stars can be used. The combination of a long coherence time with a large isoplanatic angle results in a greatly increased sky coverage for an AO system, both with natural and laser guide stars[24]. An AO system at Dome C would thus provide a higher level of correction for a larger fraction of the sky, compared to any other site. Additionally, for multi-conjugate AO, the complexity (number of deformable mirrors and actuators per mirror) is significantly reduced.

A world-wide search is currently being conducted to determine the most appropriate sites for the next generation of large optical and infrared telescopes. Advantages of the Dome C atmosphere for astronomy include the very low infrared sky emission, 10–100 times lower than observed from any mid-latitude site; the high percentage (>75%) of cloud-free time[26], which is comparable with the best mid-latitude sites; the low atmospheric precipitable water vapour content, which in winter should be lower than at any other site so far investigated, resulting in significant increases in atmospheric transmission[27]; and the low aerosol and dust content of the atmosphere. Advantageous site conditions include the very low ground level wind speeds[16] and lack of seismic activity (which reduces structural requirements on telescope mounts and domes), and low levels of light pollution. These advantages of the Dome C site must be weighed against its accessibility, any associated increase in system cost resulting from this, and any engineering issues resulting from the extremely low site temperatures. Many of the benefits of Dome C are also characteristics of the other Antarctic plateau stations. The poor ground-level seeing found at the South Pole station, however, severely limits its applicability for optical astronomy. Although it is expected that the turbulence conditions at Dome A, the highest point on the Antarctic plateau at an altitude of 4,200 m, will be superior even to Dome C, the complete lack of infrastructure at this site (it has never been visited) means that Dome C may be a preferable location.

The extremely favourable seeing, the large isoplanatic angle, and the long atmospheric coherence time reported here are compelling advantages that lead us to conclude that Dome C is the best ground-based site to develop a new astronomical observatory. □

Received 19 May; accepted 9 August 2004; doi:10.1038/nature02929.

1. Racine, R. & Ellerbroek, B. L. Profiles of the night-time turbulence above Mauna Kea and isoplanatism extension in adaptive optics. *Proc. SPIE* **2534,** 248–257 (1995).
2. Sarazin, M. Astroclimatology of Paranal (European Southern Observatory, 1999); ⟨http://www.eso.org/gen-fac/pubs/astclim/paranal/index.html⟩ (1999).
3. Michel, R., Echevarria, J., Costero, R. & Harris, O. The seeing at San Pedro Mártir Observatory as measured using the DIMM method. *Rev. Mex. Astron. Astrofis.* **19,** 37–40 (2003).
4. National Astronomical Observatory of Japan. Subaru telescope seeing ⟨http://www.naoj.org/Observing/Telescope/Image/seeing.html⟩ (2003).
5. Muñoz-Tuñón, C., Vernin, J. & Varela, A. M. Night-time image quality at Roque de los Muchachos Observatory. *Astron. Astrophys. Suppl. Ser.* **125,** 183–193 (1997).
6. Travouillon, T. *et al.* Automated Shack-Hartmann seeing measurements at the South Pole. *Astron. Astrophys.* **409,** 1169–1173 (2003).
7. Marks, R. D., Vernin, J., Azouit, M., Manigault, J. F. & Clevelin, C. Measurement of optical seeing on the high Antarctic plateau. *Astron. Astrophys. Suppl. Ser.* **134,** 161–172 (1999).
8. Candidi, M. & Lori, A. Status of the Antarctic base at Dome C and perspectives for Astrophysics. *Mem. Soc. Astron. Ital.* **74,** 29–37 (2003).
9. Ashley, M. C. B. *et al.* South Pole observations of the near-infrared sky brightness. *Pub. Astron. Soc. Pacif.* **108,** 721–723 (1996).
10. Chamberlain, M. A. *et al.* Mid-infrared observing conditions at the South Pole. *Astrophys. J.* **535,** 501–511 (2000).
11. Chamberlin, R. A. & Bally, J. 225-GHz atmospheric opacity of the South Pole sky derived from continual radiometric measurements of the sky-brightness temperature. *Appl. Opt.* **33,** 1095–1099 (1994).
12. Travouillon, T., Ashey, M. C. B., Burton, M. G., Storey, J. W. V. & Lowenstein, R. F. Atmospheric turbulence at the South Pole and its implications for astronomy. *Astron. Astrophys.* **400,** 1163–1172 (2002).

13. Gillingham, P. R. Super seeing from the Australian Antarctic Territory? *ANARE Res. Notes* **88,** 290–292 (1993).
14. Marks, R. D. Astronomical seeing from the summits of the Antarctic plateau. *Astron. Astrophys.* **385,** 328–336 (2002).
15. Aristidi, E. *et al.* Antarctic site testing: first daily seeing monitoring at Dome C. *Astron. Astrophys.* **406,** L19–L22 (2003).
16. Aristidi, E. *et al.* Preliminary summer site testing study based on weather balloons at Dome C, Antarctica. *Astron. Astrophys.* (submitted).
17. Lawrence, J. S., Ashley, M. C. B. & Storey, J. W. V. A remote, autonomous laboratory for Antarctica with hybrid power generation. *J. Electron. Electric. Eng. Aust.* (in the press).
18. Kornilov, V. *et al.* MASS: a monitor of the vertical turbulence distribution. *Proc. SPIE* **4839,** 837–845 (2003).
19. Tokovinin, A., Baumont, S. & Vasquez, J. Statistics of turbulence profile at Cerro Tololo. *Mon. Not. R. Astron. Soc.* **340,** 52–58 (2003).
20. Tokovinin, A., Kornilov, V., Shatsky, N. & Voziakova, O. Restoration of turbulence profile from scintillation indices. *Mon. Not. R. Astron. Soc.* **343,** 891–899 (2003).
21. Tokovinin, A. Measurement of seeing and atmospheric time constant by differential scintillations. *Appl. Opt.* **41,** 957–964 (2002).
22. Travouillon, T., Burton, M. G., Storey, J. W. V., Vernin, J. & Azouit, M. Comparison and cross-calibration of SODAR and microthermal sensor results. *Geophys. Res. Lett.* (submitted).
23. Chanin, M. An exceptional situation in the Antarctic stratosphere in 2002. *Mem. Soc. Astron. Ital. Suppl.* **2,** 19–25 (2003).
24. Ellerbroek, B. L. & Tyler, D. W. Adaptive optics sky coverage calculations for the Gemini-North telescope. *Publ. Astron. Soc. Pacif.* **110,** 165–185 (1998).
25. Beckers, J. M. Adaptive optics for astronomy: principles, performance, and applications. *Annu. Rev. Astron. Astrophys.* **31,** 13–62 (1993).
26. Ashley, M. C. B., Burton, M. G., Calisse, P. G., Phillips, A. & Storey, J. W. V. Site testing at Dome C—cloud statistics from the ICECAM experiment. *Highlights of Astronomy* (ASP Conf. Ser. Vol. 13, Astronomical Society of the Pacific, in the press).
27. Lawrence, J. S. Infrared and submillimeter atmospheric characteristics of high Antarctic Plateau sites. *Publ. Astron. Soc. Pacif.* **116,** 482–492 (2004).
28. National Optical Astronomy Observatory. MASS data access ⟨http://139.229.11.21/massindex.php?Submit2=MASS+Database⟩ (2004).
29. Avila, R. *et al.* Optical turbulence and wind profiles at San Pedro Martir. *Rev. Mex. Astron. Astrofis.* **19,** 11–22 (2003).
30. Vernin, J. & Muñoz-Tuñón, C. Optical seeing at La Palma Observatory. II. Intensive site testing campaign at the Nordic Optical Telescope. *Astron. Astrophys.* **284,** 311–318 (1994).

Acknowledgements The AASTINO project is supported by the Australian Research Council, the Australian Antarctic Division, the French and Italian Antarctic research programs (IPEV, PNRA) and the US National Science Foundation. The Dome C MASS is a collaboration between UNSW, CTIO and JPL. We thank J. Storey, A. Moore and C. Bonner for contributions during Dome C deployments; J. Storey, M. Swain, J. Lloyd, and J. Everett for intellectual input into the Dome C MASS project; S. Kenyon for assistance with data analysis; and V. Kornilov and N. Shatsky for software support of MASS. We also thank P. Gillingham for his encouragement over the past decade to demonstrate the existence of exceptional seeing from the Antarctic plateau.

Authors' contributions J.S.L. and M.C.B.A. designed and operated the Antarctic MASS instrumentation and co-wrote this Letter. A.T. provided the MASS sensor in collaboration with V. Kornilov *et al.* and assisted with the data analysis. T.T. assisted with the SODAR data and installation of MASS at Dome C.

Competing interests statement The authors declare that they have no competing financial interests.

Correspondence and requests for materials should be addressed to M.C.B.A. (m.ashley@unsw.edu.au).

Magnetic trapping of rare-earth atoms at millikelvin temperatures

Cindy I. Hancox, S. Charles Doret, Matthew T. Hummon, Linjiao Luo & John M. Doyle

Department of Physics, Harvard University, Cambridge, Massachusetts 02138, USA

The ability to create quantum degenerate gases has led to the realization of Bose–Einstein condensation of molecules[1–4], atom–atom entanglement[5] and the accurate measurement of the Casimir force in atom–surface interactions[6]. With a few exceptions[7–9], the achievement of quantum degeneracy relies on evaporative cooling of magnetically trapped atoms to ultracold temperatures. Magnetic traps confine atoms whose electronic magnetic moments are aligned anti-parallel to the magnetic field. This alignment must be preserved during the collisional thermalization of the atomic cloud. Quantum degeneracy has been reached in spherically symmetric, S-state atoms (atoms with zero internal orbital angular momentum). However, collisional relaxation of the atomic magnetic moments of non-S-state atoms (non-spherical atoms with non-zero internal orbital angular momentum) is thought to proceed rapidly. Here we demonstrate magnetic trapping of non-S-state rare-earth atoms, observing a suppression of the interaction anisotropy in collisions. The atoms behave effectively like S-state atoms because their unpaired electrons are shielded by two outer filled electronic shells that are spherically symmetric. Our results are promising for the creation of quantum degenerate gases with non-S-state atoms, and may facilitate the search for time variation of fundamental constants[10–12] and the development of a quantum computer with highly magnetic atoms[13].

Capturing atoms in a magnetic trap requires precooling to millikelvin temperatures. Laser cooling, the dominant method for precooling, has been used for atoms with strong cycling transitions at technologically accessible wavelengths. An alternative method is buffer-gas cooling, which relies upon collisional thermalization with a cold helium buffer gas. Although collisions with buffer gas atoms drive thermalization and subsequent trapping of the atomic cloud, they may also induce reorientation of the magnetic moment of trapped atoms (Zeeman relaxation). As only atoms in the higher-energy low-field-seeking states are trapped, the Zeeman relaxation leads to trap loss.

Evaporative cooling and buffer-gas loading have so far been limited to S-state atoms. The electronic density distribution of S-state atoms is spherically symmetric and the electrostatic interaction between atoms is not effective in driving relaxation of the highest-energy Zeeman levels in S-state atom collisions. However, if one or both of the colliding atoms have non-zero electronic orbital angular momentum (non-S-state atoms), the electronic interaction between the atoms is anisotropic[14]. The atomic angular momentum can be strongly coupled to the rotational motion of the collision complex and it has been shown that for the non-S-state atoms

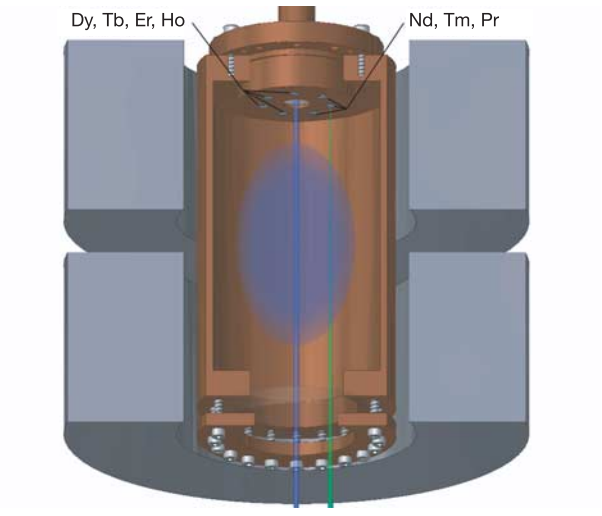

Figure 1 The experimental cell. The copper cell is thermally anchored to a dilution refrigerator. Two superconducting solenoids surround the cell. Their currents may be run in same direction to produce a uniform magnetic field, or in opposite directions to produce a spherical quadrupole trap with a depth of up to 3.5 T. The cell is filled with a buffer gas of He atoms at a density of $8 \times 10^{15}\,\mathrm{cm}^{-3}$. The rare-earth atoms are produced by laser ablation of elemental foil targets mounted at the top of the cell. The atoms are detected via absorption spectroscopy.